V.3. Slurry Reactor Kinetic Studies

The kinetics of the Fischer–Tropsch (FT) and water–gas shift (WGS) reactions were studied for four different catalysts in the slurry reactor systems. The goal of these tests was to use existing rate models from the literature for the FT and WGS reactions, fit them to our data and obtain parameter estimates, and determine which models best described our experimental results. The catalysts considered were: 100 Fe/0.3 Cu/0.2 K (Run SA–05–2957), 100 Fe/0.3 Cu/0.5 K (Run SB–07–0458, H_2 reduced), the commercial Ruhrchemie LP 33/81 catalyst (Run SA–99–0888), and 100 Fe/5.0 Cu/4.2 K/24 SiO_2 (Run SB–66–2468). The results from the first two runs were given in section V.2.3, whereas results from the last two runs can be found in section VI.3 of this report.

The data used to estimate the kinetic parameters are summarized in Tables V.3–1 through V.3–4, respectively, for each of the four runs. Only selected balances were used to estimate kinetic parameters. During Run SA–05–2957, catalyst activity was increasing during the initial portion of the run due to incomplete activation, and balances 1–7 were not included in the data set. Also, balance 12 of this run had poor closures, and was excluded as well. The initial periods of the other three runs were also excluded as catalyst activity was not stable during these periods: balances 1–4 of SB–07–0458, balances 1–6 of SA–99–0888, and balances 1–4 of SB–66–2468.

V.3.1. Kinetics Background

Stoichiometry and Reaction Rates

The FT synthesis can be approximated as a pair of simultaneous series–parallel reactions for the FT reaction and the WGS:

$$CO + (1 - m/2n)H_2 \xrightarrow{r_{FT}} \frac{1}{n}C_nH_m + H_2O \qquad \text{FT} \qquad (V.3-1)$$

$$CO - H_2O \overset{r_{WGS}}{=} CO_2 - H_2 \qquad \text{WGS} \qquad (V.3-2)$$

where n is the average carbon chain length of the hydrocarbon product and m is the average number of hydrogen atoms per hydrocarbon molecule. Both n and m vary with the catalyst and process conditions, and were determined experimentally from the gas and liquid product analyses for each balance. In these four tests, n varied between 3.45–6.14 for the 100 Fe/0.3 Cu/0.2 K catalyst, 3.68–4.23 for the 100 Fe/5.0 Cu/4.2 K/24 SiO_2 catalyst, 4.36–6.00 for the 100 Fe/0.3 Cu/0.5 K catalyst, and 3.18–3.64 for the Ruhrchemie catalyst. The ratio of m / n was less sensitive, and varied between 2.16–2.42, 2.28–2.36, 2.16–2.22, and 2.27–2.36, respectively.

Table V.3 1. Summary of kinetic data for Run SA-05-2057 (100 Fe/0.3 Cu/0.2 K catalyst).

Balance	8	9	10	11	13	14	15	16	17	18
T (°C)	220	235	250	250	265	250	250	250	250	250
P (*MPa*)	1.48	1.48	1.48	1.48	1.48	0.79	1.48	1.48	2.24	2.96
SV ($N\ell/g \cdot cat \cdot h$)	2.00	2.11	2.03	4.07	2.24	1.12	1.00	2.00	3.00	4.00
Feed H_2/CO	0.67	0.69	0.71	0.72	0.71	0.67	0.68	1.06	1.03	1.03
CO Conversion (%)	21.3	42.8	76.2	50.2	83.6	57.9	84.7	82.0	80.8	78.8
(H_2+CO) Conversion (%)	20.5	40.6	70.2	49.4	76.8	58.9	84.7	67.1	68.8	66.1
(H_2/CO) Usage	0.60	0.61	0.58	0.69	0.67	0.70	0.68	0.69	0.72	0.70
$P_{CO_2}P_{H_2}/P_{CO}P_{H_2O}$	3.5	5.6	18.8	9.7	23.5	25.2	94.6	63.1	27.2	17.2
P_{CO} (*MPa*)	0.813	0.677	0.376	0.638	0.262	0.323	0.321	0.220	0.380	0.539
P_{CO_2} (*MPa*)	0.086	0.239	0.580	0.319	0.668	0.223	0.815	0.492	0.739	0.900
P_{H_2} (*MPa*)	0.550	0.514	0.427	0.476	0.371	0.202	0.218	0.608	0.875	1.206
P_{H_2O} (*MPa*)	0.017	0.033	0.035	0.024	0.040	0.006	0.006	0.022	0.062	0.117
n	5.72	5.10	6.14	5.10	3.57	3.52	4.72	3.45	3.66	4.01
m/n	2.18	2.20	2.16	2.19	2.37	2.33	2.25	2.42	2.38	2.33

Table V.3 2. Summary of kinetic data for Run SB-07 0458 (100 Fe/0.3 Cu/0.5 K catalyst).

Balance	5	6	7	8	9	10
TOS (h)	236	284	332	380	428	452
T (°C)	250	265	265	235	250	265
P (MPa)	1.48	1.48	1.48	1.48	1.48	2.96
SV (Nℓ/g cat·h)	1.00	2.03	1.02	1.02	2.05	2.05
Feed H_2/CO	0.74	0.70	0.72	0.71	1.06	0.73
CO Conversion (%)	42.2	53.0	74.4	27.1	40.7	79.2
(H_2+CO) Conversion (%)	39.1	48.4	69.0	25.2	31.2	73.0
(H_2/CO) Usage	0.61	0.55	0.60	0.59	0.58	0.59
$P_{CO_2}P_{H_2}/P_{CO}P_{H_2O}$	10.9	25.8	39.7	10.8	13.5	25.3
P_{CO} (MPa)	0.645	0.586	0.379	0.737	0.523	0.681
P_{CO_2} (MPa)	0.246	0.330	0.598	0.156	0.180	1.205
P_{H_2} (MPa)	0.535	0.511	0.410	0.556	0.731	0.844
P_{H_2O} (MPa)	0.019	0.011	0.016	0.011	0.019	0.059
n	5.24	4.68	4.76	6.00	4.95	4.36
m/n	2.19	2.21	2.20	2.16	2.20	2.22

Table V.3 3. Summary of kinetic data for Run SA-99 0888 (Ruhrchemie LP 33/81 catalyst).

Balance	7	8	9	10	11	12	13
T (°C)	250	235	235	265	250	250	250
P (MPa)	1.48	1.48	1.48	1.48	1.48	1.48	2.96
SV ($N\ell/g$ cat·h)	1.00	2.01	1.00	2.00	2.02	2.02	4.03
Feed H_2/CO	0.65	0.65	0.67	0.67	0.67	1.00	1.02
CO Conversion (%)	56.0	18.8	30.6	57.3	32.8	48.5	36.6
(H_2+CO) Conversion (%)	56.1	23.0	35.8	56.9	35.9	45.4	39.8
(H_2/CO) Usage	0.66	1.01	0.95	0.65	0.83	0.87	1.20
$P_{CO_2}P_{H_2}/P_{CO}P_{H_2O}$	2.5	0.4	0.7	4.4	1.1	2.0	0.6
P_{CO} (MPa)	0.605	0.847	0.788	0.584	0.768	0.530	1.258
P_{CO_2} (MPa)	0.316	0.052	0.124	0.350	0.138	0.182	0.172
P_{H_2} (MPa)	0.319	0.481	0.428	0.400	0.455	0.595	1.156
P_{H_2O} (MPa)	0.080	0.071	0.096	0.055	0.072	0.105	0.268
n	3.55	3.51	3.64	3.37	3.34	3.18	3.61
m/n	2.30	2.27	2.27	2.34	2.31	2.36	2.30

Table V.3–4. Summary of kinetic data for Run SB–66–2468 (100 Fe/5.0 Cu/4.2 K/24 SiO_2 catalyst).

Balance	5	6	7
TOS (h)	453	500	549
T (°C)	250	250	250
P (MPa)	1.48	1.48	1.48
SV (Nℓ/g-cat·h)	2.00	4.00	1.00
Feed H_2/CO	0.69	0.69	0.69
CO Conversion (%)	42.3	22.3	61.0
(H_2+CO) Conversion (%)	44.3	26.2	61.1
(H_2/CO) Usage	0.78	0.99	0.76
$P_{CO_2}P_{H_2}/P_{CO}P_{H_2O}$	1.51	0.89	2.73
P_{CO} (MPa)	0.695	0.817	0.522
P_{CO_2} (MPa)	0.202	0.080	0.367
P_{H_2} (MPa)	0.441	0.499	0.391
P_{H_2O} (MPa)	0.085	0.055	0.101
n	4.23	3.90	3.68
m/n	2.28	2.28	2.36

Water is generally believed to be the primary byproduct of the FT reaction, and CO_2 is produced by the WGS (Dry et al, 1972). The small amount of oxygenated products, primarily alcohols, and the CO_2 formed by the Boudouard reaction, ($2CO - C(s) + CO_2$), are neglected in the scheme given by Equations V.3–1 and V.3–2. The WGS is particularly important over potassium promoted iron catalysts, which can have significant shift activity. In some cases, the WGS may approach equilibrium during the reaction (Huff and Satterfield, 1984 a, b; Nettelhoff et al, 1985; Bukur and Brown, 1987).

The uniform temperature, pressure, and concentrations achieved in a slurry stirred tank reactor simplifies calculation of reaction rates. Assuming that the reactor is at steady state, the rates of the FT and WGS reactions are given by:

$$r_{FT} = \left(\frac{P_S}{RT_S}\right)^s \frac{f_{H_2-CO}}{2 - m/2n} \qquad (V.3-3)$$

$$r_{WGS} = \left(\frac{P_S}{RT_S}\right)^s \frac{1 - m/2n - U}{(1-U)(2 + m/2n)} f_{H_2-CO} \qquad (V.3-4)$$

Note that the rate of syngas consumption (H_2–CO) differs from the FT reaction rate only by stoichiometry, $(-r_{H_2-CO}) = (2 - m/2n)r_{FT}$, and that the FT and WGS reaction rates are related by the H_2/CO usage ratio and stoichiometry.

Reaction rates are functions of temperature and liquid phase concentrations in a slurry reactor. Assuming that the gas and liquid phase concentrations are in equilibrium, the gas phase is ideal, and that the gaseous species obey Henry's Law in the liquid phase, partial pressures may be used in the rate equations in place of liquid concentrations or activities. Henry's Law behavior in typical slurry liquids for the principal products and reactants of the FT synthesis (CO, CO_2, H_2, H_2O) has been reported in the literature (e.g., Peter and Weinert, 1955; Albal et al, 1984; Matsumoto and Satterfield, 1985; Huang et al, 1988). Preliminary calculations showed that the gas phase behaved ideally. We assumed that the average hydrocarbon product (C_nH_m) had the physical properties of propylene, and were able to estimate the gas phase fugacity coefficients in the mixture using the Redlich–Kwong equation of state. The values estimated for the fugacity coefficients were better than 1.00 ± 0.05 for all species at all conditions employed in this report. Under these conditions, the partial pressures and liquid concentrations can be related directly: $C_{l,j} = H_j P_j$. The use of liquid concentrations, activities, or partial pressures may effect the dimensions of some constants in the rate expression. Furthermore, since Henry's constants are functions of temperature, activation energies may change when different concentration terms are used. If the Henry's constants are assumed to follow an

Arrhenius temperature dependence, their activation energies are in the range −10.8 to 4.6 kJ / mol (Nettelhoff et al, 1985). In this report, we base our estimates using partial pressures in the rate equations. Also, literature values of rate constants were converted to our units for consistency, however, reported activation energies were not adjusted to account for the temperature dependence of the Henry's Law constants.

Kinetic Models

The first order dependence of the FT reaction rate on H_2 partial pressure is well known:

$$r_{FT} = k_1 P_{H_2} \qquad (V.3-5)$$

Anderson (1956, pp 283–297) found that the first order rate fit the data well, up to $H_2 \div CO$ conversions of 60 %. The activation energies from the precipitated catalysts tested by Pichler (reported by Anderson) were 87 kJ / mol, and for the fused or precipitated catalysts tested at the U. S. Bureau of Mines, 84 and 87 kJ / mol. Nitrided fused iron catalysts had activation energies in the range 80–88 kJ / mol. Dry et al (1972) studied a fused, promoted iron catalyst in a differential fixed bed reactor, and found that the reaction rate was first order in H_2 partial pressure. The activation energy was 70 kJ / mol. Under the conditions of their study (i.e., low conversions) no rate dependence on CO partial pressure was observed.

Rate inhibition by water can occur at higher conversions (> 60 %). Anderson (1956) proposed a rate equation which included water inhibition, which had the form:

$$r_{FT} = \frac{k_0 P_{CO} P_{H_2}}{P_{CO} - a P_{H_2O}} \qquad (V.3-6)$$

Dry (1976) was able to derive this equation from the enol mechanism (Storch et al, 1951, pp 581–593) by assuming that the hydrogenation of chemisorbed CO was the rate determining step:

$$A_j + M \overset{K_j}{=} \begin{matrix} A_j \\ | \\ M \end{matrix} \qquad (V.3-7)$$

$$\begin{matrix} CO \\ | \\ M \end{matrix} + H_2 \xrightarrow{k_0} \begin{matrix} COH_2 \\ | \\ M \end{matrix} \qquad (V.3-8)$$

where we have used | to denote a bond of indefinite order.

Dry assumed Langmuir adsorption, and considered competitive adsorption of CO, CO_2, H_2, and H_2O. Assuming that the fraction of sites covered by the active intermediate COH_2 is small, then the surface fraction of CO is given by:

$$\theta_{CO} = \frac{K_{CO} P_{CO}}{1 + K_{CO} P_{CO} - K_{CO_2} P_{CO_2} - K_{H_2} P_{H_2} + K_{H_2O} P_{H_2O}} \qquad (V.3-9)$$

and the rate from Equation V.3–8 is:

$$r_{FT} = k_0\theta_{CO}P_{H_2} = \frac{k_0K_{CO}P_{CO}}{1 - K_{CO}P_{CO} + K_{CO_2}P_{CO_2} + K_{H_2}P_{H_2} + K_{H_2O}P_{H_2O}} \qquad (V.3-10)$$

He further suggested that $K_{CO}P_{CO} + K_{H_2O}P_{H_2O} \gg 1 + K_{CO_2}P_{CO_2} + K_{H_2}P_{H_2}$ to arrive at the expression given by Equation V.3–6, with $a = K_{H_2O} / K_{CO}$.

Atwood and Bennett (1979) used Equation V.3–6 for data taken over a fused, nitrided ammonia synthesis catalyst (CCI). Water inhibition was important only at the highest temperatures and conversions. They determined the activation energy of k_0 to be 85 kJ / mol, and for the adsorption term, a, –0 kJ / mol. (In our work, we assume that all constants appearing in the rate expressions follow an Arrhenius temperature dependence). Huff and Satterfield (1984a) found that the adsorption term a decreased linearly with H_2 partial pressure. A commercial fused iron ammonia synthesis catalyst was used in their work as well (United Catalysts, Inc., C–73). Anderson (1956) also mentioned that the rate constants appearing in Equation V.3–6 showed trends with feed composition.

To account for this dependence, Huff and Satterfield were able to derive an alternate rate form, using two different mechanisms: the carbide mechanism, assuming that the hydrogenation of surface carbon was the rate determining step, and an enol/carbide mechanism, with the hydrogenation of surface enol as the rate determining step. The carbide mechanism proposes that CO adsorbs dissociatively to form an active surface carbon species. Methylene groups formed by the hydrogenation of the surface carbon polymerize to produce hydrocarbons, and water is produced via the reaction of hydrogen with surface oxygen:

$$CO + 2M \overset{K^d_{CO}}{=\!=} \underset{M}{C} - \underset{M}{O} \qquad (V.3-11)$$

$$\underset{M}{O} - H_2 \overset{K_1}{=\!=} H_2O - M \qquad (V.3-12)$$

$$\underset{M}{C} + H_2 \xrightarrow{k_0} \underset{M}{CH_2} \qquad (V.3-13)$$

Assuming that the fraction of sites covered by the methylene groups is small, the surface coverage of active carbon is given by:

$$\theta_C = \frac{K^d_{CO}K_1P_{CO}P_{H_2}}{K^d_{CO}K_1P_{CO}P_{H_2} + (1 + \frac{P_{H_2O}}{K_1P_{H_2}})P_{H_2O}} \qquad (V.3-14)$$

Assuming that $1 + P_{H_2O} / K_1 P_{H_2} \approx 1$, then the rate can be written from Equation V.3–13 as:

$$r_{FT} = \frac{k_0 P_{CO} P_{H_2}^2}{P_{CO} P_{H_2} + b P_{H_2O}} \qquad (V.3-15)$$

where $b = 1 / K_{CO}^d K_1$. The assumption that $1 + P_{H_2O} / K_1 P_{H_2} \approx 1$ is the same as assuming the surface fraction of O to be very small.

The combined enol/carbide mechanism proposes that the methylene groups are formed by eliminating water from the enol in the rate limiting step:

$$\underset{M}{CO} + H_2 \overset{K_2}{=\!=} \underset{M}{COH_2} \qquad (V.3-16)$$

$$\underset{M}{COH_2} + H_2 \xrightarrow{k_0} \underset{M}{CH_2} - H_2O \qquad (V.3-17)$$

Considering the adsorption of species per Equation V.3–7, the surface concentration of the enol intermediate is given by:

$$\theta_{COH_2} = \frac{K_2 K_{CO} P_{CO} P_{H_2}}{K_2 K_{CO} P_{CO} P_{H_2} + 1 + K_{CO} P_{CO} - K_{CO_2} P_{CO_2} + K_{H_2} P_{H_2} + K_{H_2O} P_{H_2O}} \qquad (V.3-18)$$

If H_2O adsorbs strongly compared to the other species, such that $K_2 K_{CO} P_{CO} P_{H_2} + K_{H_2O} P_{H_2O} \gg 1 + K_{CO} P_{CO} + K_{CO_2} P_{CO_2} + K_{H_2} P_{H_2}$, then the rate equation has the same form as Equation V.3–15, where b is now given by $K_{H_2O} / K_2 K_{CO}$. Furthermore, Equations V.3–6 and V.3–15 have the same form if the constant a (Equation V.3–6) is a function of H_2 partial pressure, i.e., $a = b / P_{H_2}$.

For the data of Huff and Satterfield (1984a), Equation V.3–15 gave a better fit. In order to obtain as good a correlation using Equation V.3–6, a constant term had to be included in the denominator. The activation energy for the FT rate constant, k_0, was 83 kJ / mol. Nettelhoff et al (1985) considered both Equations V.3–6 and V.3–15 for their data taken over a precipitated, unpromoted iron catalyst. At 270 °C, both rate forms agreed reasonably well with their data, although Equation V.3–6 gave a slightly higher statistical correlation (the R^2 correlation coefficient was 0.99 for Equation V.3–6 and 0.95 for Equation V.3–15). At conversions below 60 %, the rate was first order, with an activation energy of 89 kJ / mol.

Inhibition by CO_2 is generally not as strong as inhibition by water due to the large adsorption coefficient of water relative to CO and CO_2. In slurry reactors, inhibition by water is further enhanced by its high solubility in typical slurry reactor waxes. However, CO_2 inhibition may

become important when a large fraction of the water produced from the FT reaction reacts with CO to produce CO_2 via the WGS (Equation V.3–2). This situation may occur when the catalyst has high WGS activity and/or low H_2/CO feed ratios are employed. Ledakowicz et al (1985) derived a rate expression which incorporated inhibition by CO_2 from the enol mechanism (Equations V.3–7–10), but assumed that CO_2 was the dominant term in the denominator of Equation V.3–10 (thus $K_{CO}P_{CO} + K_{CO_2}P_{CO_2} \gg 1 + K_{H_2}P_{H_2} + K_{H_2O}P_{H_2O}$). Their rate expression was then given by:

$$r_{FT} = \frac{k_0 P_{CO} P_{H_2}}{P_{CO} + cP_{CO_2}} \qquad (V.3-19)$$

where $c = K_{CO_2} / K_{CO}$.

For their precipitated catalyst (100 Fe/1.3 K), which showed high WGS activity, most of the water produced from the FT synthesis subsequently reacted to form CO_2. Catalyst activity, particularly at higher temperatures, did not follow first order kinetics. The constant c in Equation V.3–19 was estimated at 0.115, and was relatively insensitive to temperature. The FT activation energy was 103 kJ / mol. Nettelhoff et al (1985) considered Equation V.3–19 for a commercial fused iron ammonia synthesis catalyst (BASF S5–10). This catalyst also had high WGS activity, and did not show inhibition by product water.

A summary of the rate forms and parameter estimates for the FT reaction appearing in the recent literature is given in Table V.3–5. Some conclusions can be drawn from the previous studies: (1) The activation energy for the FT reaction was about 80–103 kJ / mol, regardless of catalyst type, in these recent studies. This is within the range 63–105 kJ / mol of Huff and Satterfield (1984a) who reviewed a broader range of reaction studies; (2) Water inhibited the rate more strongly than CO_2. CO_2 inhibition was overshadowed by water inhibition, except when the WGS reaction consumed most of the water produced by the FT reaction; (3) All of the proposed FT rate expressions reduced to first order in H_2 partial pressure at low conversions. This simple relationship can be used below conversions in the range 40–70 % in a stirred tank reactor (Huff and Satterfield, 1984b).

To account for inhibition by both water and CO_2, Ledakowicz et al (1985) proposed a general kinetic model which has the same form as either Equations V.3–6 or V.3–19, and is obtained directly from Equation V.3–10 assuming that both water and CO_2 are significant terms in the denominator. (thus $K_{CO}P_{CO} - K_{CO_2}P_{CO_2} - K_{H_2O}P_{H_2O} \gg 1 - K_{H_2}P_{H_2}$):

$$r_{FT} = \frac{k_0 P_{CO} P_{H_2}}{P_{CO} - aP_{H_2O} - cP_{CO_2}} \qquad (V.3-20)$$

Table V.3-5. Summary of FT kinetic expressions and parameter values from the literature.

Atwood and Bennett (1979)	CCI fused iron	$r_{FT} = \frac{k_0 P_{CO} P_{H_2}}{P_{CO} + a P_{H_2O}}$	T (°C)	$k_0^{(a)}$	n
			250	0.0017	0.028
			282	0.0049	0.028
			315	0.013	0.028
			E (kJ/mol)	85	−8.8
Leib and Kuo (1984)	Fe/Cu/K	$r_{FT} = \frac{k_0 P_{CO} P_{H_2}}{P_{CO} + a P_{H_2O}}$	T (°C)	$k_0^{(a)}$	a
			265	0.062	0.58
Nettelhoff et al. (1985)	Precipitated Fe	$r_{FT} = \frac{k_0 P_{CO} P_{H_2}}{P_{CO} + a P_{H_2O}}$	T (°C)	$k_0^{(a)}$	a
			270	0.018	4.51
			E (kJ/mol)	89	
Huff and Satterfield (1984a)	C 73 fused iron (United Catalysts, Inc.)	$r_{FT} = \frac{k_0 P_{CO} P_{H_2}^2}{P_{CO} P_{H_2} + b P_{H_2O}}$	T (°C)	$k_0^{(a)}$	b (MPa)
			232	0.013	2.56
			248	0.025	1.15
			263	0.042	0.67
			E (kJ/mol)	83	−100
Nettelhoff et al. (1985)	S6-10 fused iron (BASF)	$r_{FT} = \frac{k_0 P_{CO} P_{H_2}}{P_{CO} + c P_{CO_2}}$	T (°C)	$k_0^{(a)}$	c
			240	0.010	0.19
			E (kJ/mol)	81	
Ledakowicz et al. (1985)	Precipitated 100 Fe/1.3 K	$r_{FT} = \frac{k_0 P_{CO} P_{H_2}}{P_{CO} + c P_{CO_2}}$	T (°C)	$k_0^{(a)}$	c
			220	0.0088	0.255
			240	0.025	0.210
			250	0.049	0.229
			260	0.058	0.237
			E (kJ/mol)	103	0

(a) Units of k_0 are mol/g-cat-h-MPa

This generalized rate expression may be used for catalysts with low WGS activity, where water concentrations are high, as well as for catalysts with high shift activity which show inhibition by CO_2.

The WGS is important for slurry processing since it enables CO rich feeds to be utilized efficiently without the need for an external shift. Both Equations V.3–1 and V.3–2 for the FT and WGS reactions must be considered to accurately predict both H_2+CO conversions and H_2/CO usage ratios, which requires knowledge of WGS kinetics. The shift reaction occurs readily over potassium promoted iron catalysts, such as those considered here, and may approach equilibrium in some situations. There have only been a few studies of WGS kinetics in conjunction with the FT synthesis reported in the literature. Kuo (1983) and Leib and Kuo (1984) considered mass action kinetics for the WGS, with a denominator shared with their FT rate expression, which had the form of Equation V.3–6:

$$r_{WGS} = \frac{k_{w.0}(P_{CO}P_{H_2O} - P_{CO_2}P_{H_2} / K_P)}{P_{CO} + aP_{H_2O}} \qquad (V.3-21)$$

Bohlbro (1969, pp 27–34) derived a rate expression for the WGS from the reactions of CO and H_2 with oxidized surface sites (Kulkova and Temkin mechanism):

$$CO + \underset{M}{O} \underset{k_{-f}}{\overset{k_f}{=}} CO_2 + M \qquad (V.3-22)$$

$$H_2O + M \underset{k_{-r}}{\overset{k_r}{=}} H_2 + \underset{M}{O} \qquad (V.3-23)$$

He assumed that the surface concentration of oxygen was described by a Langmuir isotherm. The numerator of the rate equation followed mass action kinetics, while the denominator contained terms for CO, CO_2, H_2, and H_2O:

$$r_{WGS} = \frac{k_r(P_{CO}P_{H_2O} - P_{CO_2}P_{H_2} / K_P)}{P_{CO} + \frac{k_{-f}}{k_f}P_{CO_2} + \frac{k_r}{k_f}P_{H_2O} + \frac{k_{-r}}{k_f}P_{H_2}} \qquad (V.3-24)$$

This expression has the same form as Equation V.3–21 if it is assumed that $P_{CO} - \frac{k_r}{k_f}P_{H_2O} \gg \frac{k_{-f}}{k_f}P_{CO_2} - \frac{k_{-r}}{k_f}P_{H_2}$, where $k_{w.0} = k_r$ and $a = k_r/k_f$. The constants appearing in the denominator of Equation V.3–24 are rate constants, not adsorption coefficients, and the definition of a from Equation V.3–24 differs from the definition using the FT rate expression, Equation V.3–6. Also, there are differences in the surface species and sites between a WGS catalyst and an FT

catalyst, however, it seems reasonable that for the purpose of kinetics, the FT and WGS rate equations can share the same form of denominator, as was used by Kuo.

Feimer et al (1981) used a first order in CO rate equation for the WGS:

$$r_{WGS} = k_w P_{CO} \qquad (V.3-25)$$

They studied a potassium and copper promoted, precipitated iron catalyst (100 Fe/20 Cu/0.8 K), and determined an apparent activation energy of 124 kJ / mol for the WGS. Equation V.3–25 can be derived from Equation V.3–21 when the partial pressure of water is large relative to CO and CO_2, or when water is strongly adsorbed and the reverse WGS reaction is negligible.

V.3.2. Results and Discussion

First Order Kinetics

The first order rate constants for the four catalysts were estimated by plotting the FT reaction rate against the H_2 partial pressure. These plots are shown in Figure V.3–1 for the unsupported catalysts (100 Fe/0.3 Cu/0.2 K, 100 Fe/0.3 Cu/0.5 K) and Figure V.3–2 for the silica–containing catalysts (100 Fe/5.0 Cu/4.2 K/24 SiO_2, Ruhrchemie). The rate constant, k_1, on this type of plot was calculated as the slope of the best line through the origin. The estimated rate constants for the four catalysts are shown on an Arrhenius diagram in Figure V.3–3, and are compared numerically in Table V.3–6. Catalyst activity was highest for the 100 Fe/0.3 Cu/0.2 K catalyst, followed by the 100 Fe/5.0 Cu/4.2 K/24 SiO_2 catalyst, the Ruhrchemie catalyst, and the 100 Fe/0.3 Cu/0.5 K catalyst . The activation energies for the 100 Fe/0.3 Cu/0.2 K and Ruhrchemie catalysts were both 86 kJ / mol , which is within the range expected from the literature. The activation energy for the 100 Fe/0.3 Cu/0.5 K catalyst was higher, 102 kJ / mol, which is still within the expected range. The activation energy for the 100 Fe/5.0 Cu/4.2 K/24 SiO_2 catalyst was not calculated since data were available at only a single temperature (250 °C). This simple rate expression fit the data fairly accurately for all four catalysts at the conditions employed during our tests.

Inhibition by Water

The effect of water inhibition on the catalysts was evaluated considering Equations V.3–6 and V.3–15. The range of H_2O partial pressures measured in Run SA–05–2957 (100 Fe/0.3 Cu/0.2 K) was 0.006–0.117 MPa and in Run SB–07–0458 (100 Fe/0.3 Cu/0.5 K) was 0.011–0.059 MPa, which at similar process conditions were generally lower than those encountered during Run SA–99–0888 (Ruhrchemie), 0.055–0.268 MPa and SB–66–2468 (100 Fe/5.0 Cu/4.2

Table V.3 6. Summary of FT first order rate constants.

Run	SA-05-2057		SB-07-0458		SA-09-0888		SB-00-2468	
Catalyst	100 Fe/0.3 Cu/0.2 K		100 Fe/0.3 Cu/0.2 K		Ruhrchemie LP 33/81		100 Fe/5 Cu/4.2 K/24 SiO_2	
T (°C)	$k_0^{(1)}$	RMSE	$k_0^{(1)}$	RMSE	$k_0^{(1)}$	RMSE	$k_0^{(1)}$	RMSE
220	0.011	(2)	–	–	–	–	–	–
235	0.024	(2)	0.0007	(2)	0.013	0.049	–	–
250	0.035	0.100	0.012	0.058	0.020	0.029	0.027	0.070
265	0.065	(2)	0.026	0.025	0.040	(2)	–	–
E (kJ/mol)	86.6	–	102	–	85.7	–	(2)	–

(1) Units of k_0 are mol/g-cat-h-MPa
(2) Only 1 data point available

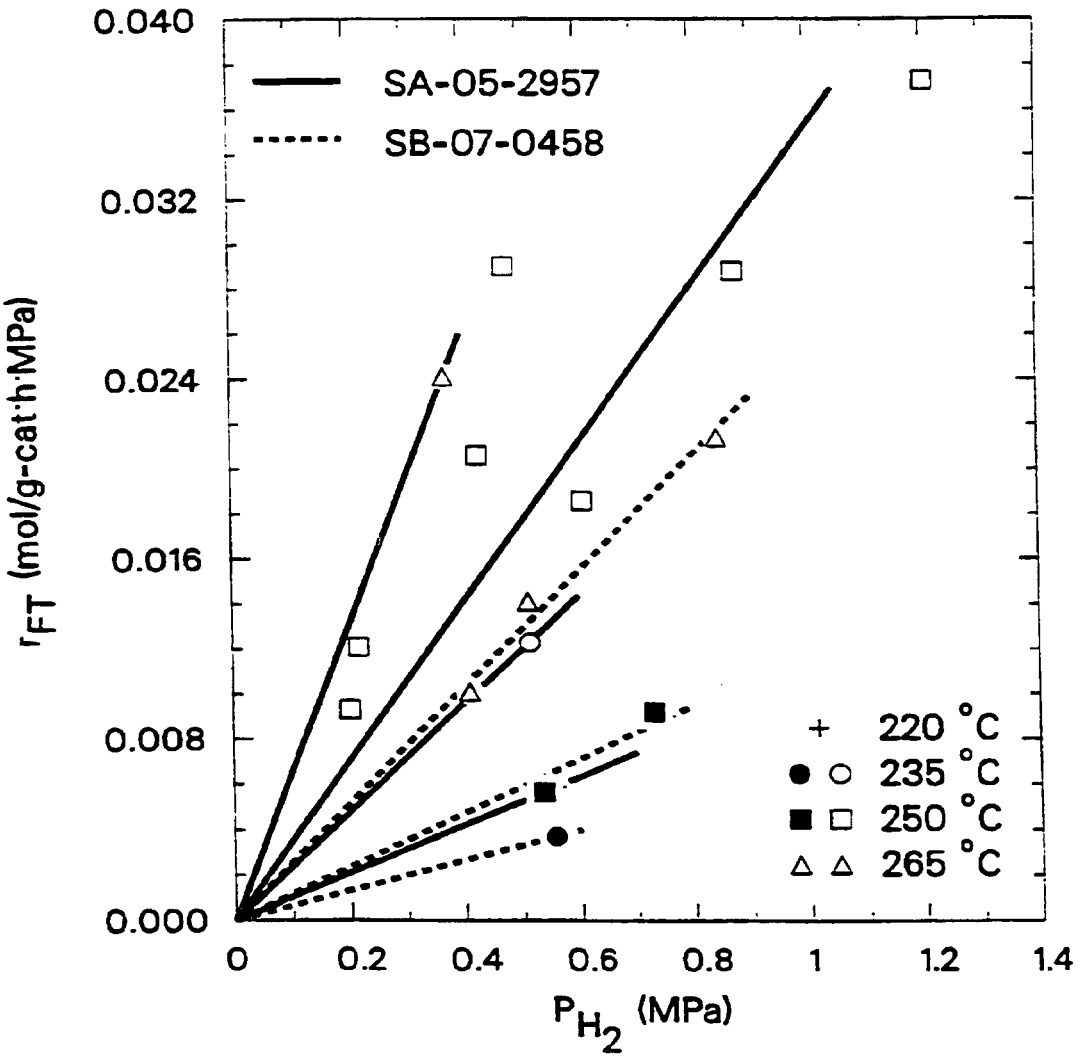

Figure V.3-1. FT first order plot for the 100 Fe/0.3 Cu/0.2 K (SA-05-2957) and 100 Fe/0.3 Cu/0.5 K (SB-07-0458) catalysts.

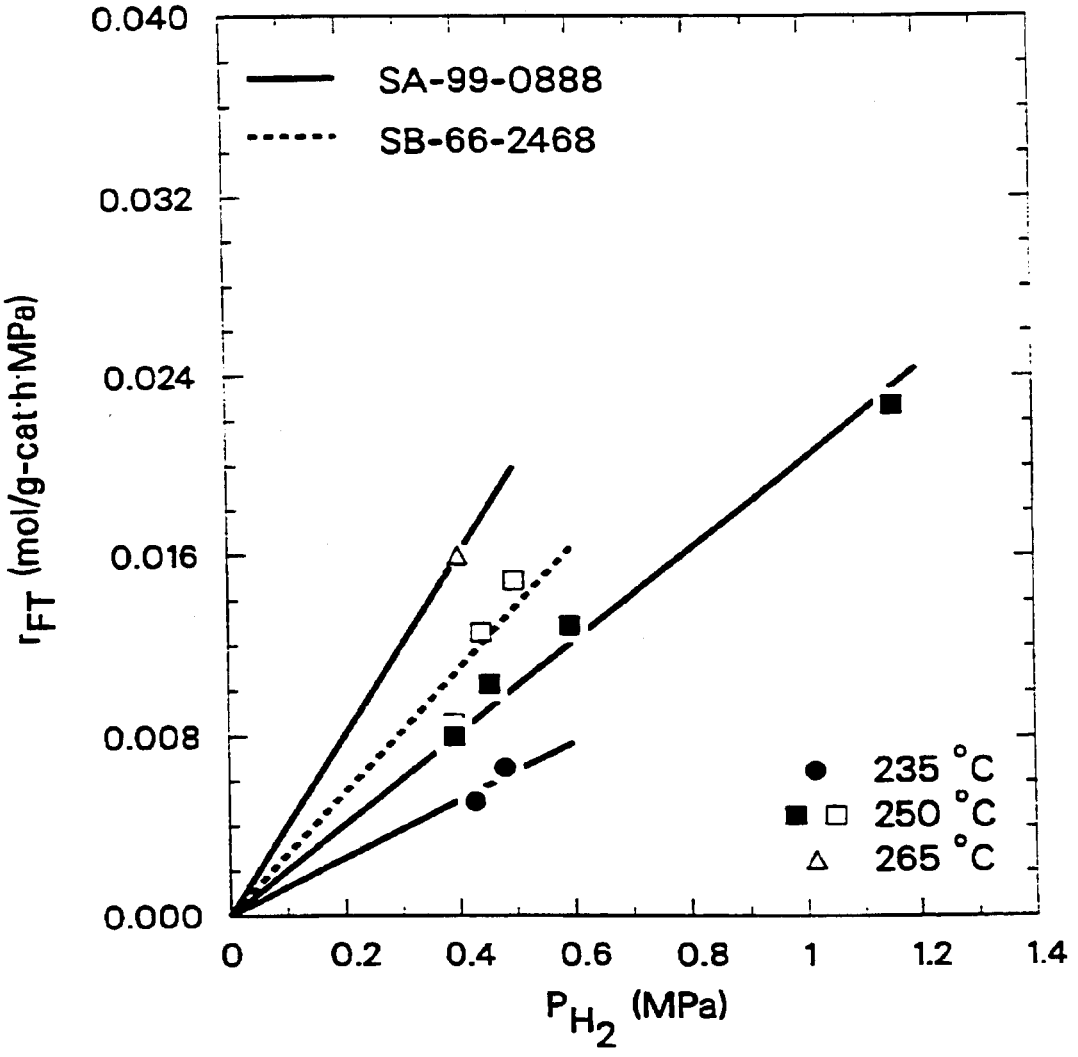

Figure V.3-2. FT first order plot for the Ruhrchemie LP 33/81 (SA-99-0888) and 100 Fe/5.0 Cu/4.2 K/24 SiO_2 (SB-66-2468) catalysts.

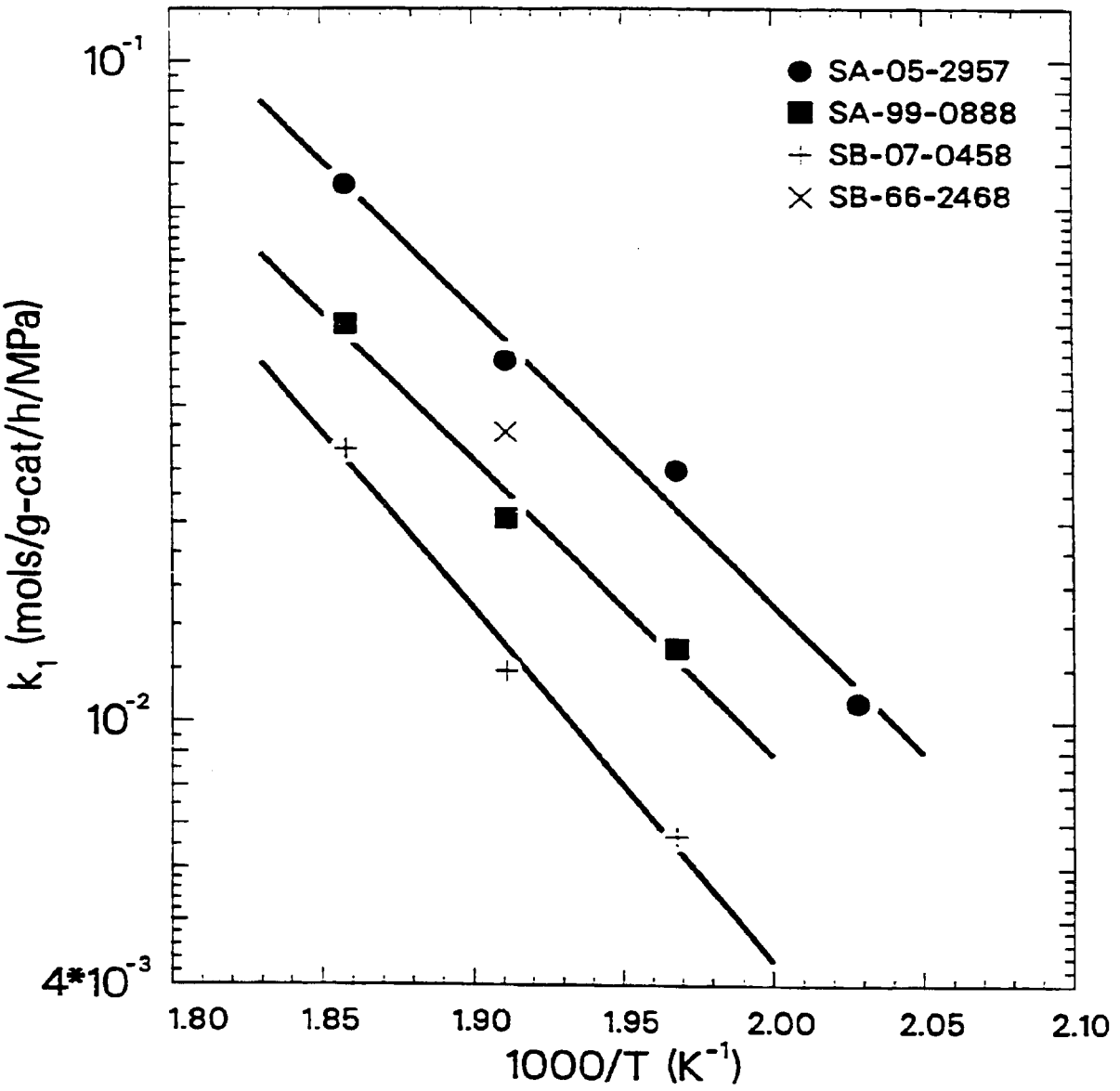

Figure V.3-3. Arrhenius plot of the FT first order rate constants.

K/24 SiO_2), 0.055–0.101 MPa. Huff and Satterfield (1984a) indicated that inhibition was not important below water partial pressures of 0.1–0.15 MPa for their fused catalyst.

Equations V.3–6 and V.3–15 can be linearized as:

$$P_{H_2} / r_{FT} = \frac{1}{k_0} + \frac{a}{k_0} \frac{P_{H_2O}}{P_{CO}} \qquad (V.3-26)$$

$$P_{H_2} / r_{FT} = \frac{1}{k_0} + \frac{b}{k_0} \frac{P_{H_2O}}{P_{CO} P_{H_2}} \qquad (V.3-27)$$

Plotting the data in this form, P_{H_2} / r_{FT} versus P_{H_2O}/P_{CO} (Equation V.3–26) or $P_{H_2O}/P_{CO}P_{H_2}$ (Equation V.3–27), should give a straight line which has an intercept $1 / k_0$ and a slope a / k_0 (Equation V.3–26) or b / k_0 (Equation V.3–27). The constants were calculated from the least squares slope and intercept of the linearized equation for all of Equations V.3–6, V.3–15, and V.3–19. The constants estimated in this manner for all four catalysts are summarized in Table V.3–7. The linear plot of Equation V.3–6 for the four catalysts is shown in Figure V.3–4. The Ruhrchemie and 100 Fe/0.3 Cu/0.5 K catalysts show only mild inhibition by water, with $a = 0.73$ and 0.99, respectively. The weak effect of water on the reaction rate may be due to the low conversions and/or the low H_2O partial pressures obtained under the reaction conditions employed in this study. The H_2–CO conversions varied between 35.9–56.1 % for the points shown for Ruhrchemie catalyst. The 100 Fe/0.3 Cu/0.2 K catalyst was more active than the Ruhrchemie catalyst, and the conversions and H_2O partial pressures were higher. A stronger inhibition effect was seen for this catalyst ($a = 4.2$), as well as for the 100 Fe/5.0 Cu/4.2 K/24 SiO_2 catalyst ($a = 3.9$). Catalyst activity followed the same trend seen with the first order rate constants: 100 Fe/0.3 Cu/0.2 K > 100 Fe/5.0 Cu/4.2 K/24 SiO_2 > Ruhrchemie > 100 Fe/0.3 Cu/0.5 K. The results shown for the 100 Fe/0.3 Cu/0.5 K catalyst are at 265 °C, but it has comparable activity to the Ruhrchemie catalyst at 250 °C. For each catalyst, k_0 was greater than the first order rate constant k_1 (0.035, 0.027, 0.020, and 0.026 mol / g–cat·h, respectively). This was expected since k_1 is an apparent rate constant, which incorporates inhibition by water and/or CO_2 (i.e., the denominators of Equations V.3–6, V.3–15, V.3–19, or V.3–20).

The linear plot of Equation V.3–15 is shown in Figure V.3–5. Equation V.3–15 gave a poorer fit to the data for the 100 Fe/0.3 Cu/0.2 K catalyst, and the normalized root mean square error (RMSE) value was 0.077 using Equation V.3–15 and 0.058 for Equation V.3–6 (Figure V.3–4). We use the RMSE to compare model predictions of reaction rates to the

Table V.3-7. Summary of FT kinetic parameter estimates.

Run	SA-05-2957	SB-07-0458	SA-99-0888	SB-60-2408
Catalyst	100 Fe/0.3 Cu/0.2 K	100 Fe/0.3 Cu/0.5 K	Ruhrchemie LP 33/81	100 Fe/5 Cu/4.2 K/24 SiO_2
T (°C)	260	265	250	250
Eq. (V.3-6)				
$k_0^{(1)}$	0.057	0.027	0.023	0.039
a	4.2	0.90	0.73	3.9
RMSE	0.058	0.020	0.021	0.030
Eq. (V.3-15)				
$k_0^{(1)}$	0.073	0.029	0.021	0.036
b	5.5	1.6	-- 0.049	1.3
RMSE	0.077	0.0093	0.031	0.027
Eq. (V.3-19)				
$k_0^{(1)}$	0.054	0.029	0.021	0.033
c	0.21	0.09	0.036	0.69
RMSE	0.096	0.0095	0.035	0.010
Eq. (V.3-20)				
$k_0^{(1)}$	0.066	(2)	0.024	(2)
a	4.6		0.80	
c	0.13		0.08	
RMSE	0.047		0.023	

(1) Units of k_0 are mol/g-cat-h-MPa

(2) Zero or negative parameter estimates

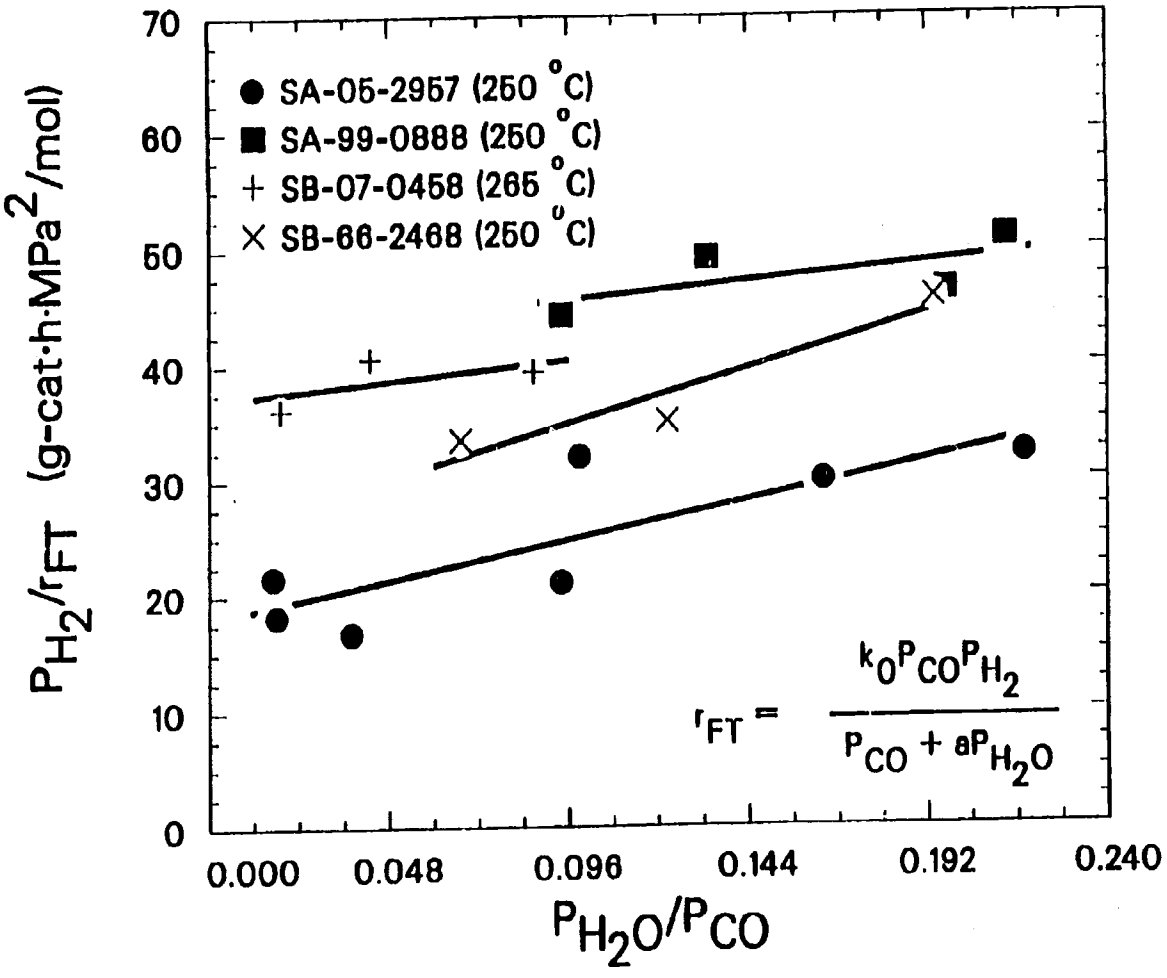

Figure V.3-4. Linear plot of the FT rate expression given by Equation V.3-6 (H_2O inhibition).

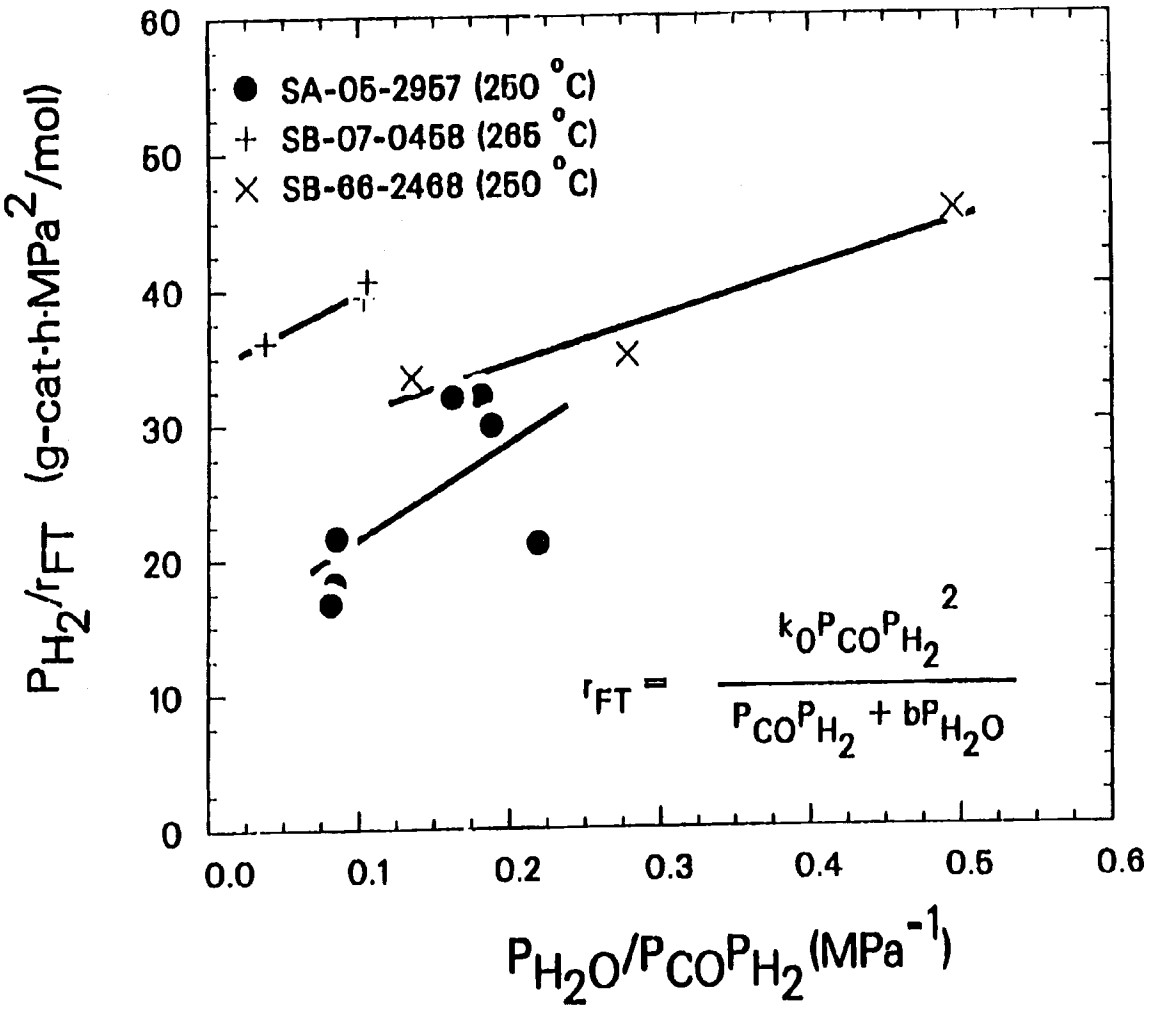

Figure V.3-5. Linear plot of the FT rate expression given by Equation V.3-15 (H_2O inhibition).

experimental values, and have defined RMSE as:

$$\text{RMSE} = \frac{\sqrt{\sum_{i=1}^{N}(r_{k,i}^{meas} - r_{k,i}^{calc})^2}}{N r_{k,avg}^{meas}} \qquad (V.3-28)$$

The fit for the 100 Fe/5.0 Cu/4.2 K/24 SiO_2 catalyst was approximately the same, with RMSE values of 0.030 (Equation V.3–6) and 0.027 (Equation V.3–15), while the 100 Fe/0.3 Cu/0.5 K catalyst showed a strong improvement, RMSE = 0.020 (Equation V.3–6) and 0.0093 (Equation V.3–15). The 100 Fe/0.3 Cu/0.2 K catalyst showed the strongest water inhibition effect and gave b = 5.5 MPa, compared to b = 1.3 MPa for the 100 Fe/5.0 Cu/4.2 K/24 SiO_2 catalyst and b = 1.6 MPa for the 100 Fe/0.3 Cu/0.5 K catalyst. Water inhibition was virtually non–existent for the Ruhrchemie catalyst when Equation V.3–15 was used, and the rate constant, k_1 = 0.021 mol / g–cat-h, was nearly the same as the apparent first order rate constant, with a small negative estimate for b, – 0.049.

We can compare our results obtained using Equation V.3–6 to those of Atwood and Bennett (1979), Leib and Kuo (1984), and Nettelhoff et al (1985), who all used the same form of rate equation. The catalysts we tested were significantly more active than the fused iron catalyst used by Atwood and Bennett. Their catalyst was also less active than the other catalysts shown in Table V.3–5, which is seen by comparing k_0 values. Leib and Kuo (1983) estimated their rate constants from experiments conducted in a bubble column reactor using an Fe/Cu/K catalyst (67 weight % Fe). Their activity at higher temperature was similar to our 100 Fe/0.3 Cu/0.2 K catalyst, k_0 = 0.062 (265 °C) versus 0.057 (250 °C) mol / g–cat-h · MPa, and had a lower adsorption coefficient. The catalyst tested by Nettelhoff et al (unpromoted Fe) was also less active than the catalysts tested in our work. At 270 °C, their rate constant k_0 was less than the values obtained for our catalyst tests at 250 °C. Our higher activity may be due to the potassium promotion in the catalysts we tested. Their adsorption coefficient (a = 4.51) was similar to that for the 100 Fe/0.3 Cu/0.2 K (a = 4.2) and 100 Fe/5.0 Cu/4.2 K/24 SiO_2 catalysts (a = 3.9). The parameters estimated from Equation V.3–15 can be compared to the results of Huff and Satterfield (1984a). The Ruhrchemie catalyst had comparable activity to the fused iron catalyst used in their study, with similar first order rate constants, although we did not find any effect of water using Equation V.3–15. The 100 Fe/0.3 Cu/0.2 K catalyst was more active, and at 250 °C, its k_0 was about 2.9 times greater than that for the fused catalyst, although water inhibited the FT reaction rate more strongly for our catalyst. The 100 Fe/5.0 Cu/4.2 K/24 SiO_2 catalyst showed somewhat higher activity than the fused iron (about

1.4 times greater) with approximately the same water inhibition effect. At 265 °C, the 100 Fe/0.3 Cu/0.5 K catalyst was less active than their fused iron, with a similar H_2O adsorption coefficient.

Inhibition by CO_2

The rate expression derived by Ledakowicz et al (1985) to account for inhibition by CO_2 (Equation V.3–19) was studied in a similar manner. The linear form of Equation V.3–19 is given by:

$$P_{H_2} / r_{FT} = \frac{1}{k_0} + \frac{c}{k_0} \frac{P_{CO_2}}{P_{CO}} \qquad (V.3-29)$$

A linear plot of Equation V.3–19 is shown in Figure V.3–6. The CO_2 partial pressures during Run SA–99–0888 (Ruhrchemie) were too low, 0.052–0.350 MPa, to be used with this rate equation, and the estimate for c was nearly zero, $c = 0.036$. The data for the other three catalysts show inhibition by CO_2, and the constant c in Equation V.3–19 was estimated at 0.21, 0.69, 0.09 for the 100 Fe/0.3 Cu/0.2 K, 100 Fe/5.0 Cu/4.2 K/24 SiO_2, and 100 Fe/0.3 Cu/0.5 K catalysts, respectively. Inhibition by water was much stronger than for CO_2, and the adsorption coefficient, a, in the analogous Equation V.3–6 was about 20 times greater than that for CO_2 with the 100 Fe/0.3 Cu/0.2 K catalyst, about 6 times greater for the 100 Fe/5.0 Cu/4.2 K/24 SiO_2 catalyst, and about 11 times greater using the 100 Fe/0.3 Cu/0.5 K catalyst.

The 100 Fe/0.3 Cu/0.2 K and 100 Fe/5.0 Cu/4.2 K/24 SiO_2 catalysts were significantly more active than the S6–10 fused catalyst studied by Nettelhoff et al (1985). The 100 Fe/0.3 Cu/0.2 K catalyst had comparable activity to the 100 Fe/1.3 K catalyst used by Ledakowicz et al (1985). Our rate constant k_0 at 250 °C was approximately the same as for their catalyst, as was our estimate of the CO_2 adsorption coefficient, c. Their catalyst was more active than the 100 Fe/5.0 Cu/4.2 K/24 SiO_2 catalyst, and showed a weaker CO_2 inhibition effect. The S6–10 fused iron was significantly more active than the 100 Fe/0.3 Cu/0.5 K catalyst.

The analysis of our data for the 100 Fe/0.3 Cu/0.2 K catalyst using Equations V.3–6, V.3–15, and V.3–19 showed that both CO_2 and water potentially inhibited the reaction rate, thus we also considered Equation V.3–20, which includes inhibition by both product species. Equation V.3–20 was linearized, and the constants estimated via multiple linear regression of the 250 °C data. A parity plot of experimental and expected rates is shown in Figure V.3–7 for the 100 Fe/0.3 Cu/0.2 K and Ruhrchemie catalysts. The 100 Fe/5.0 Cu/4.2 K/24 SiO_2 and 100 Fe/0.3 Cu/0.5 K catalysts gave negative adsorption coefficients when fit to this equation,

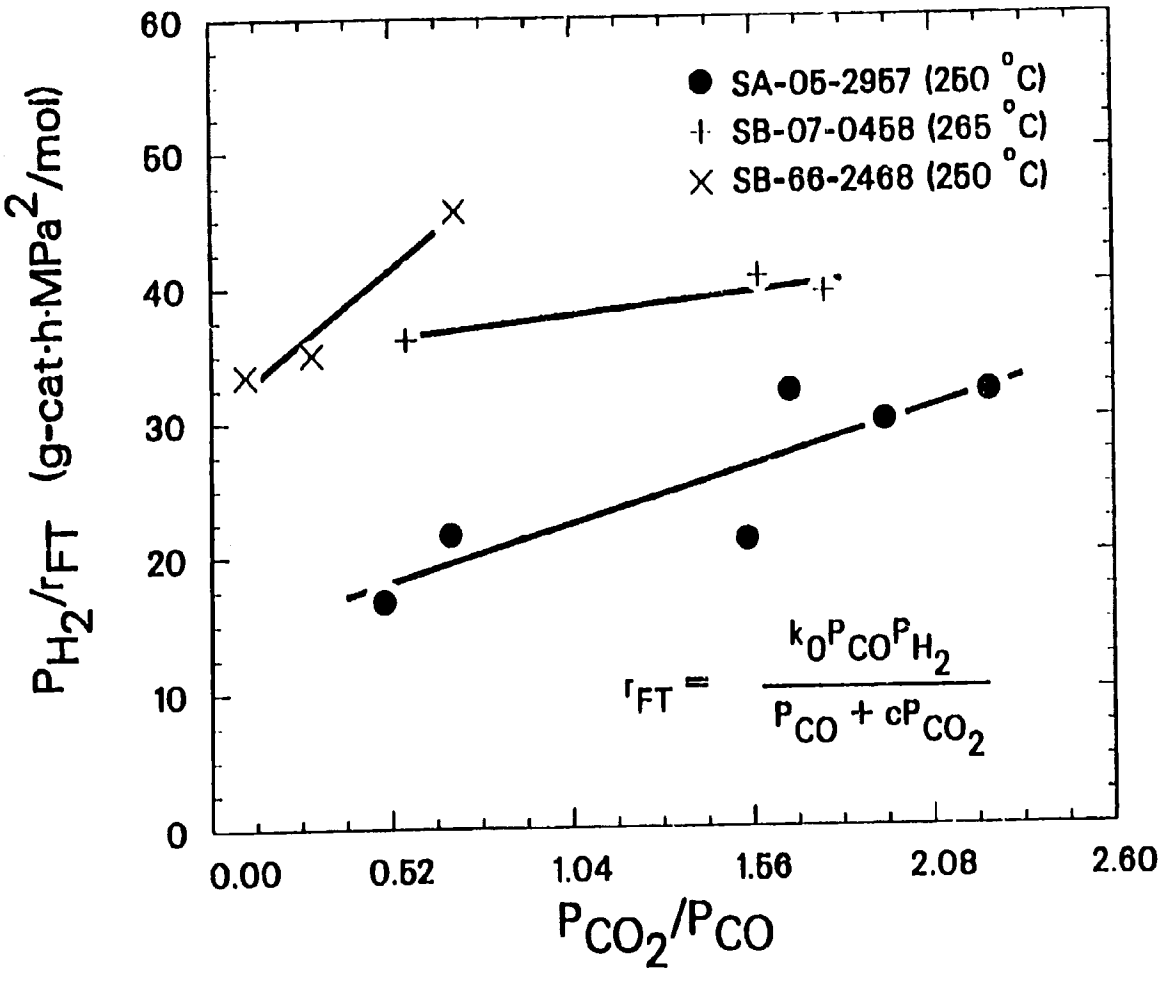

Figure V.3-6. Linear plot of the FT rate expression given by Equation V.3-19 (CO_2 inhibition).

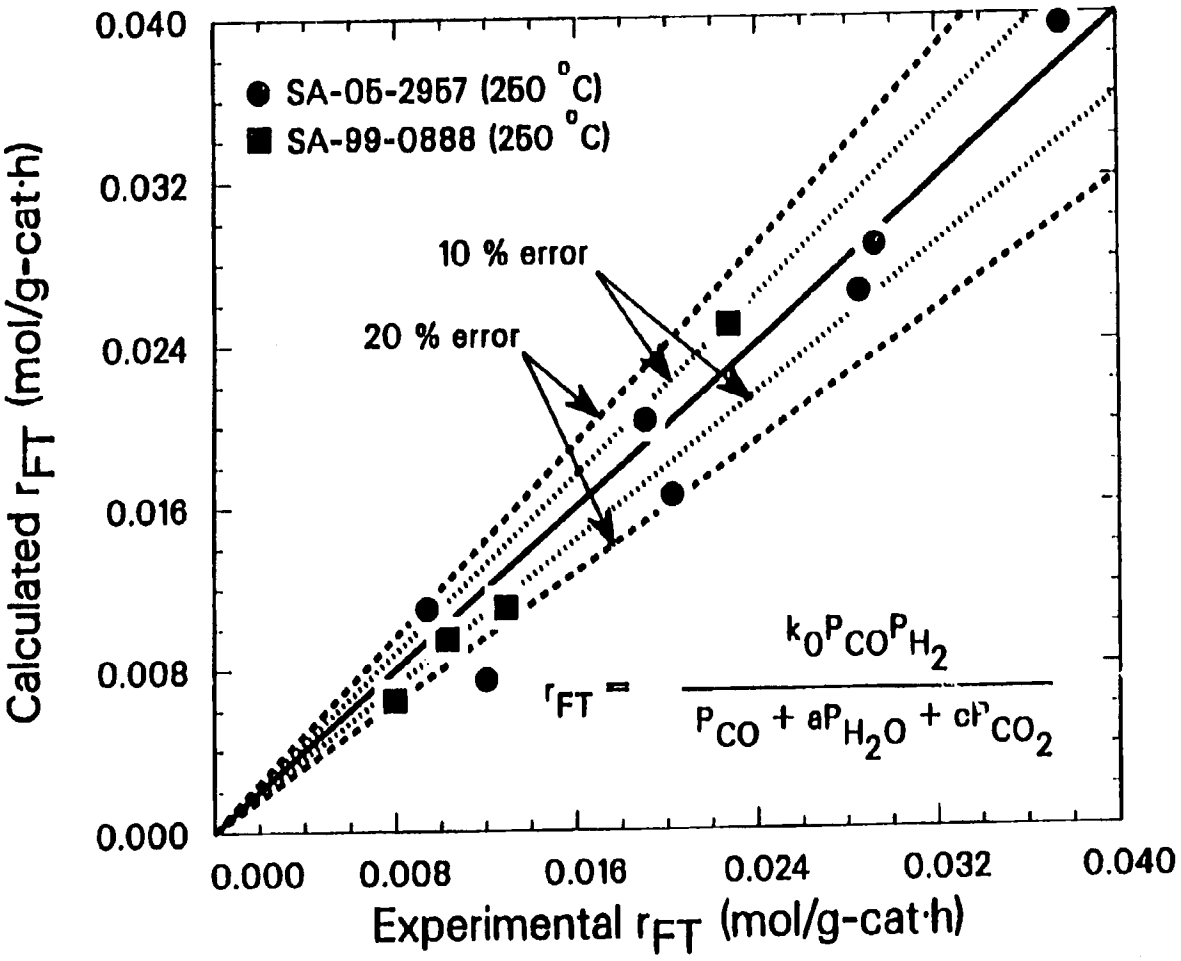

Figure V.3-7. Parity plot of the FT rate expression given by Equation V.3-20 (H_2O inhibition).

thus were not used. The negative rate constants were probably due to the few data points available for these two catalysts. In both cases, the number of data points was equal to the number of constants in the model (= 3), which makes the parameter estimates sensitive to small errors in the data. For the other two catalysts, the model fits our data, although some scatter in the data is apparent. The trends seen previously with CO_2 and water inhibition were also observed for this model. Water was adsorbed much more strongly than CO_2, and the ratio of the adsorption coefficients (a / c) was about 35 for the 100 Fe/0.3 Cu/0.2 K catalyst. However, since this catalyst has good WGS activity, the CO_2 partial pressures were high enough to cause rate inhibition. The constant c for the Ruhrchemie catalyst was nearly zero, contributing little to the denominator of Equation V.3–20.

Water – Gas Shift Kinetics

A comparison of the measured $P_{CO_2}P_{H_2}/P_{CO}P_{H_2O}$ ratios from our data to the equilibrium constant (Newsome, 1980) is shown in Figure V.3–8. The measured $P_{CO_2}P_{H_2}/P_{CO}P_{H_2O}$ ratios generally approach equilibrium at higher temperatures as the WGS reaction rate increases. The 100 Fe/0.3 Cu/0.2 K catalyst is also seen to have higher WGS activity than either the Ruhrchemie or 100 Fe/5.0 Cu/4.2 K/24 SiO_2 catalysts, and its ratios were closer to equilibrium at all temperatures. Since most of the measured points fall far away from equilibrium, it is important to consider the kinetics of the WGS.

The first order plots for the WGS reaction are shown for the 100 Fe/0.3 Cu/0.2 K and 100 Fe/0.3 Cu/0.5 K catalysts in Figure V.3–9, and for the Ruhrchemie and 100 Fe/5.0 Cu/4.2 K/24 SiO_2 catalysts in Figure V.3–10. The slope of the best line through the origin on these plots is the estimate of the rate constant. The first order in CO rate constants (Equation V.3–25) from our tests are plotted on an Arrhenius diagram in Figure V.3–11, and are compared numerically in Table V.3–8. The rate constants from the 100 Fe/0.3 Cu/0.2 K catalyst were higher than those from the other three catalysts by a factor of about 4–5, regardless of temperature. The activation energies measured for the WGS reaction were 132 kJ / mol for the 100 Fe/0.3 Cu/0.2 K and 100 Fe/0.3 Cu/0.5 K catalysts, and 137 kJ / mol for the Ruhrchemie catalyst. These values are in good agreement with the 124 kJ / mol reported by Feimer et al, who also considered first order in CO WGS kinetics.

The mass action kinetic equation (Equation V.3–21) was also used for the WGS. The rate constant $k_{w,0}$ was estimated in the following manner: using the same value of a (Equation V.3–6) obtained for the FT kinetics, Equation V.3–21 was multiplied through by the denominator of

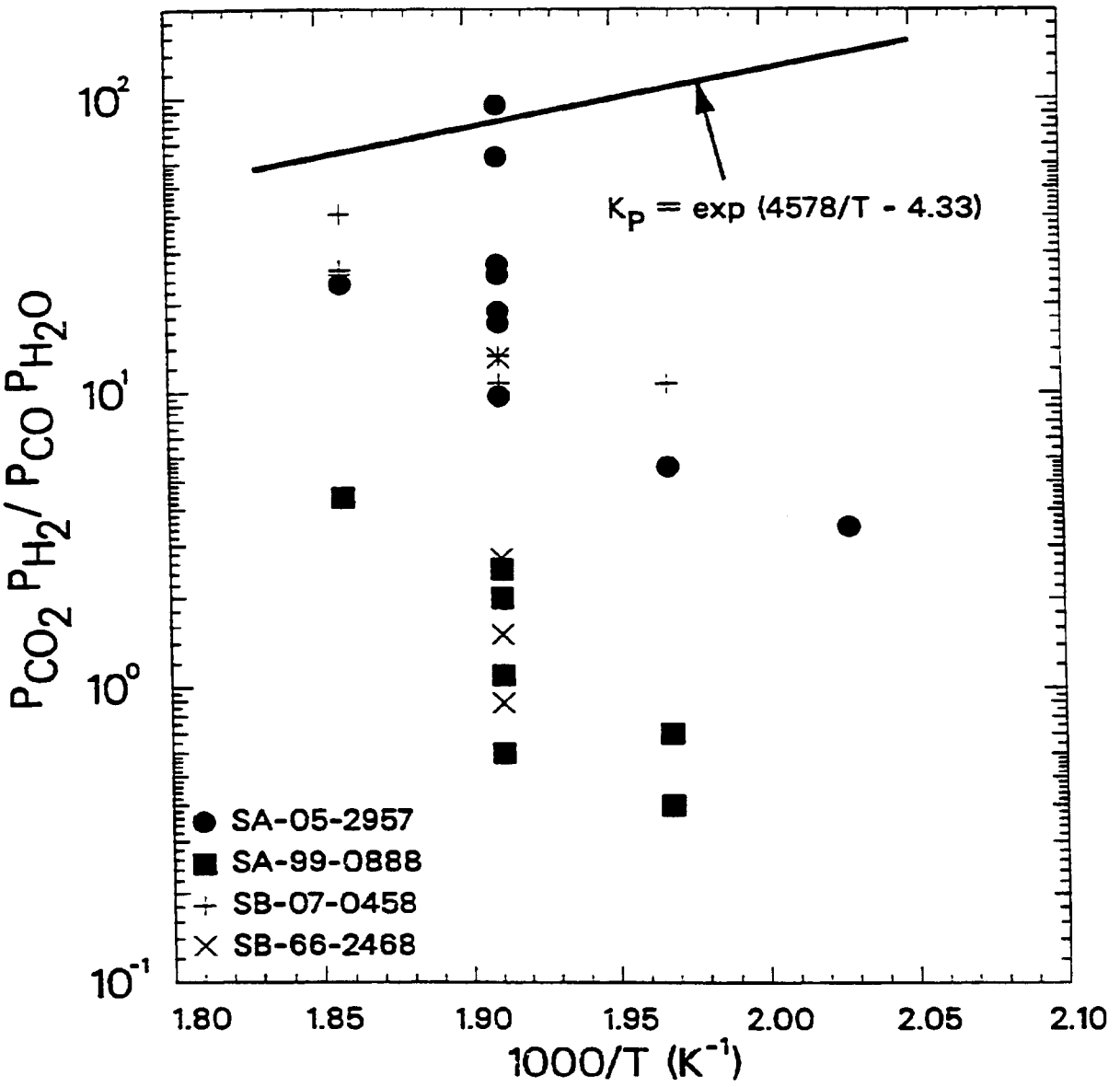

Figure V.3-8. Comparison of measured $P_{CO_2}P_{H_2}/P_{CO}P_{H_2O}$ ratios to equilibrium.

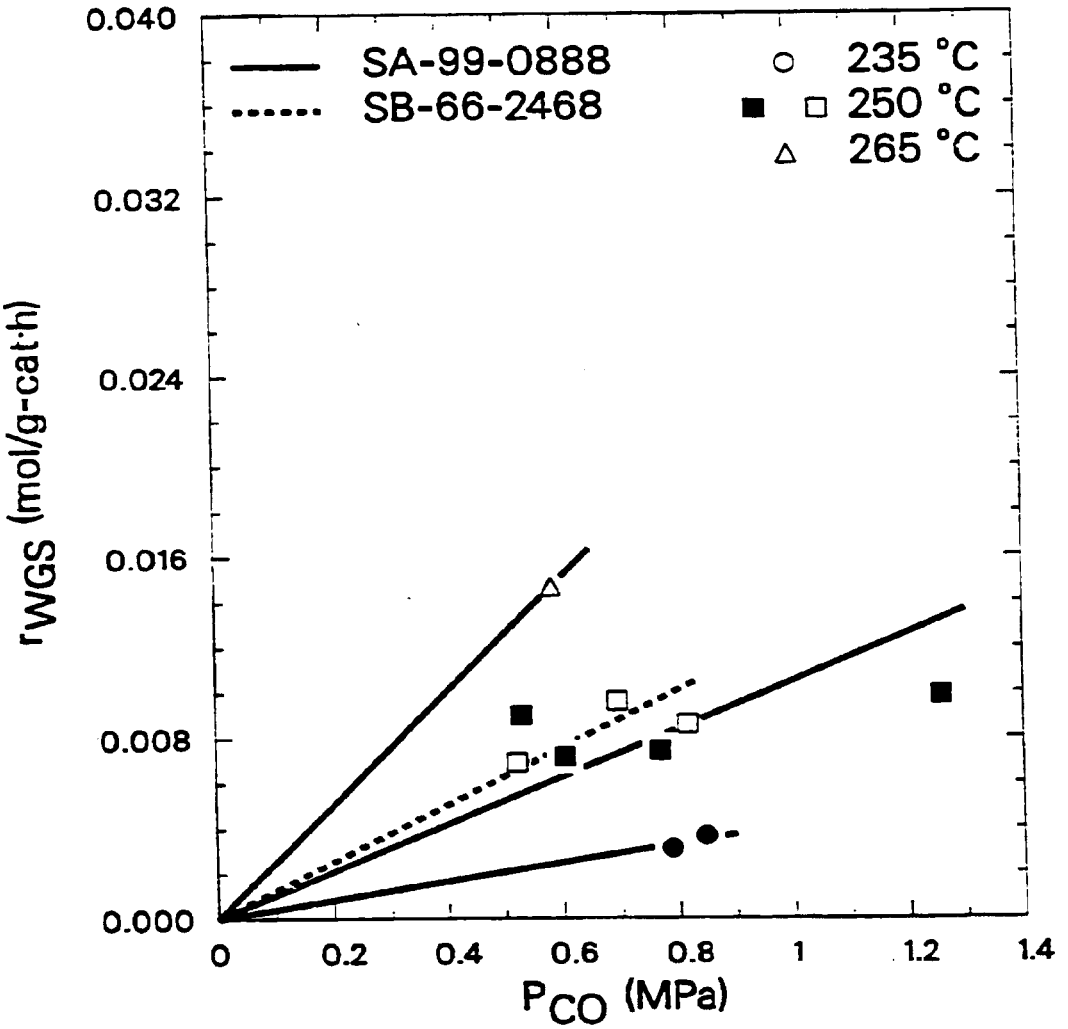

Figure V.3-9. WGS first order plot for the 100 Fe/0.3 Cu/0.2 K (SA-05-2957) and 100 Fe/0.3 Cu/0.5 K (SB-07-0458) catalysts.

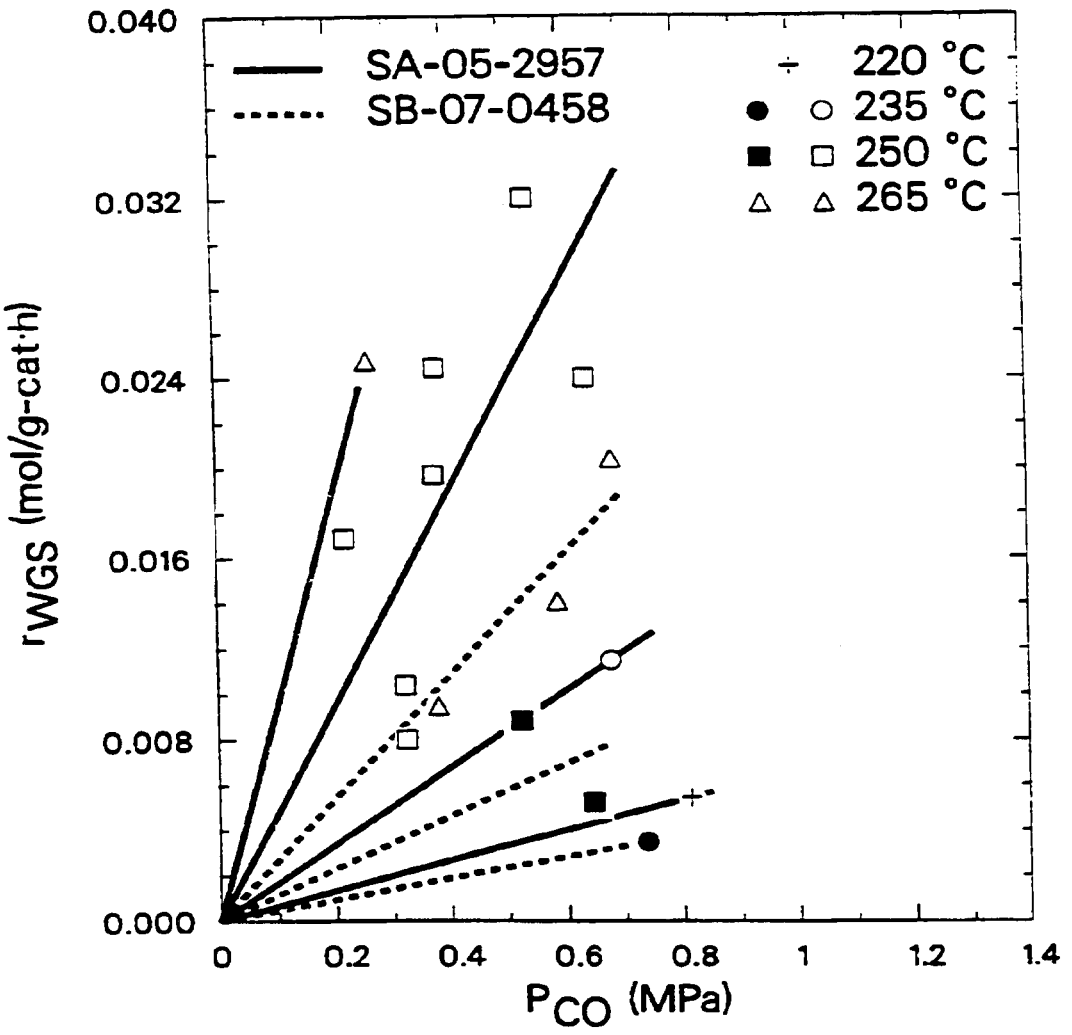

Figure V.3–10. WGS first order plot for the Ruhrchemie LP 33/81 (SA–99–0888) and 100 Fe/5.0 Cu/4.2 K/24 SiO_2 (SB–66–2468) catalysts.

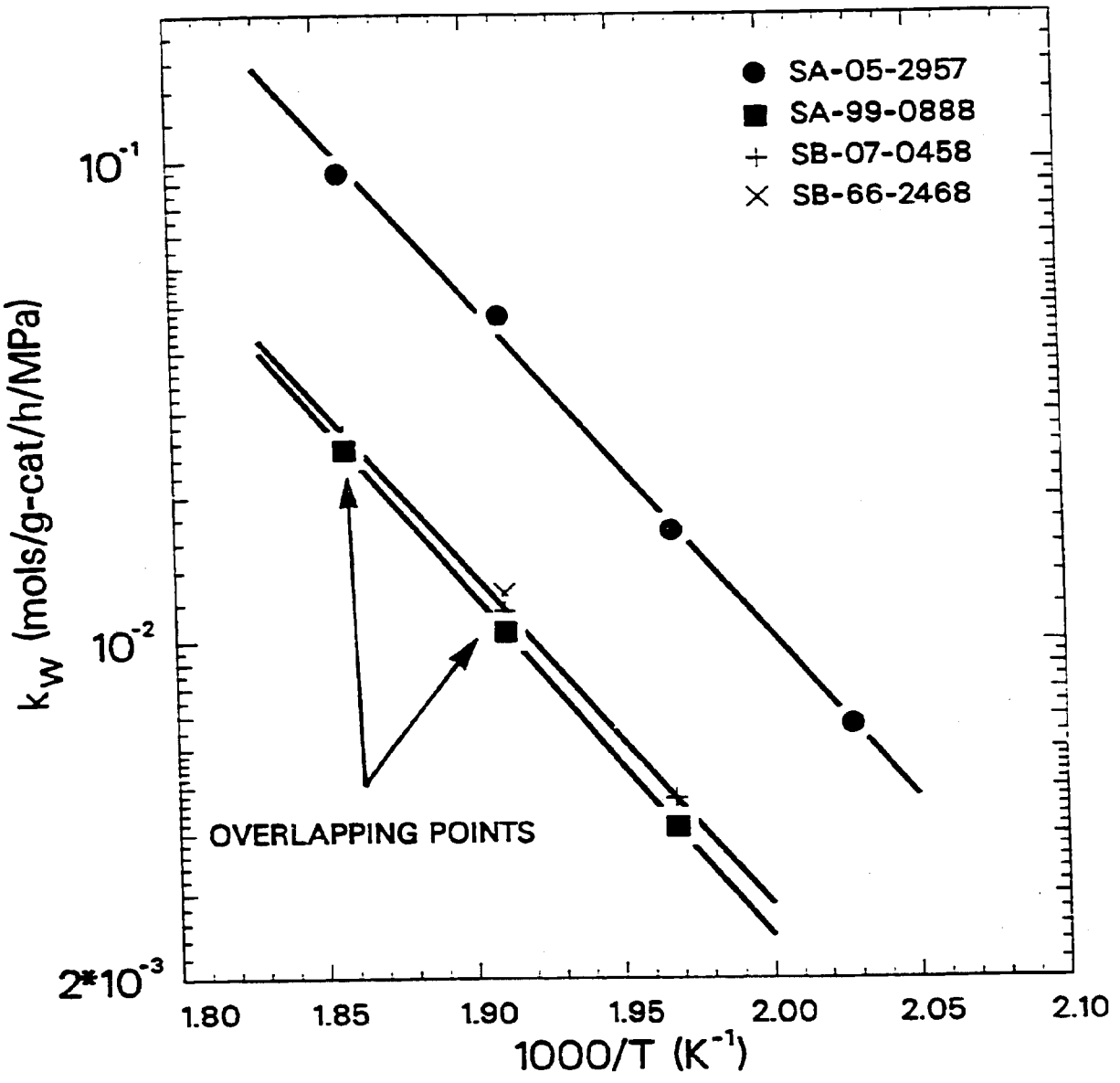

Figure V.3-11. Arrhenius plot of the WGS first order rate constants.

Table V.3-8. Summary of WGS first order rate constants.

Run	SA-05-2057		SB-07-0458		SA-99-0888		SB-66-2408	
Catalyst	100 Fe/0.3 Cu/0.2 K		100 Fe/0.3 Cu/0.5 K		Ruhrchemie LP 33/81		100 Fe/5 Cu/4.2 K/24 SiO_2	
T (°C)	$k_{w,0}^{(1)}$	RMSE	$k_{w,0}^{(1)}$	RMSE	$k_{w,0}^{(1)}$	RMSE	$k_{w,0}^{(1)}$	RMSE
220	0.0008	(2)	–	–	–	–	–	
235	0.017	(2)	0.0047	(2)	0.0042	0.301	–	
250	0.048	0.255	0.012	0.241	0.0090	0.142	0.013	0.074
265	0.095	0.078	0.027	0.209	0.025	(2)	–	–
E (kJ/mol)	132	–	132	–	136	–	(2)	–

(1) Units of $k_{w,0}$ are mol/g-cat-h-MPa
(2) Only 1 data point available

the right–hand side. The resulting equation is linear with respect to $k_{w,0}$, and the rate constant was then calculated as the slope of the best line through the origin. The WGS equilibrium constant, K_P, is a known function of temperature, $K_P = \exp(4578 / T - 4.33)$, and was not considered to be a variable kinetic parameter. We also considered mass action kinetics with the denominators of the FT rate expressions given by Equations V.3–15, V.3–19, and V.3–20 as well. The resulting WGS kinetic equations have the form:

$$r_{WGS} = \frac{k_{w,0}(P_{CO}P_{H_2O} - P_{CO_2}P_{H_2} / K_P)}{P_{CO}P_{H_2} - bP_{H_2O}} \qquad (V.3-30)$$

$$r_{WGS} = \frac{k_{w,0}(P_{CO}P_{H_2O} - P_{CO_2}P_{H_2} / K_P)}{P_{CO} - cP_{CO_2}} \qquad (V.3-31)$$

$$r_{WGS} = \frac{k_{w,0}(P_{CO}P_{H_2O} - P_{CO_2}P_{H_2} / K_P)}{P_{CO} - aP_{H_2O} - cP_{CO_2}} \qquad (V.3-32)$$

The rate constants $k_{w,0}$ for these rate forms were estimated in the same manner as described above. The results for the rate constants $k_{w,0}$ are given in Table V.3–9 for all catalysts. The fit of first order in CO kinetics was good for all catalysts. Using the 100 Fe/0.3 Cu/0.2 K catalyst, the lowest RMSE value was obtained using Equation V.3–30. The other models gave poorer fits. With the other catalysts, the first order in CO kinetics were superior to the nonlinear kinetics, based on the RMSE values. Leib and Kuo (1984) estimated $k_{w,0}$ at 0.66 mol / g–cat·h · MPa for a = 0.58 for their iron based catalyst (265 °C). Their rate constant is comparable to our estimate for the 100 Fe/0.3 Cu/0.2 K catalyst, and is higher than the constants obtained for the Ruhrchemie, 100 Fe/0.3 Cu/0.5 K, or 100 Fe/5.0 Cu/4.2 K/24 SiO_2 catalysts.

V.3.3. Summary

Several different rate forms were tested for each catalyst to model the FT and WGS reaction rates. Our results show that water inhibits the FT reaction more strongly than does CO_2, however, in all cases, the FT rates were approximately first order with respect to H_2. Using the 100 Fe/0.3 Cu/0.2 K catalyst (Run SA–05–2957), the best FT rate model contained terms for both water and CO_2 inhibition, given by Equation V.3–20. The model originally proposed by Anderson (1956), Equation V.3–6, was nearly as good, with a slightly higher RMSE. Equation V.3–6 also gave the best fit for the Ruhrchemie catalyst, although there was little actual difference between any of the models for this catalyst. The Ruhrchemie catalyst had low activity during Run SA–99–0888, which leads to low conversions and H_2O and CO_2

Table V.3 0. Summary of WGS kinetic parameter estimates.

Run	SA-05-2957	SB-07-0458	SA-99-0888	SB-66-2468
Catalyst	100 Fe/0.3 Cu/0.2 K	100 Fe/0.3 Cu/0.6 K	Ruhrchemie LP 33/81	100 Fe/5 Cu/4.2 K/24 SiO_2
T (°C)	250	265	250	250
Eq. (V.3-21)				
$k_{w,0}^{(1)}$	0.74	0.43	0.047	0.17
RMSE	0.170	0.347	0.228	0.109
Eq. (V.3-30)				
$k_{w,0}^{(2)}$	0.84	0.29	(3)	0.069
RMSE	0.144	0.370		0.164
Eq. (V.3-31)				
$k_{w,0}^{(1)}$	0.56	0.43	0.041	0.14
RMSE	0.213	0.361	0.234	0.201
Eq. (V.3-32)				
$k_{w,0}^{(1)}$	0.85	(3)	0.048	(3)
RMSE	0.169		0.230	

(1) Units of $k_{w,0}$ are mol/g-cat·h·MPa
(2) Units of $k_{w,0}$ are mol/g-cat·h
(3) FT parameters less than or equal to zero

partial pressures. Under these conditions, inhibition effects are negligible. The FT kinetic equation which accounted for CO_2 alone, Equation V.3–19, gave the best fit to the data taken over the 100 Fe/5.0 Cu/4.2 K/24 SiO_2 catalyst (Run SB–66–2468). However, since inhibition by water is much stronger than CO_2, the kinetics which include water should be considered. Both of the water inhibition models (Equations V.3–6 and V.3–15) gave a good fit to the data for this catalyst as well. The FT kinetic model proposed by Huff and Satterfield (1984a) was the best for the 100 Fe/0.3 Cu/0.5 K catalyst (Run SB–07–0458). Activation energies based on the first order rate constants were estimated to be approximately 86 kJ / mol for the 100 Fe/0.3 Cu/0.2 K and Ruhrchemie catalysts, and 102 kJ / mol for the 100 Fe/0.3 Cu/0.5 K catalyst. These estimates are in agreement with the range of activation energies reported in the literature, 80–103 kJ / mol.

The kinetics of the WGS reaction were also studied. Simple first order in CO kinetics (Equation V.3–25) was tested, and this simple model gave the best fit to the data from the 100 Fe/0.3 Cu/0.5 K, 100 Fe/5.0 Cu/4.2 K/24 SiO_2 and Ruhrchemie catalysts. For the 100 Fe/0.3 Cu/0.2 K catalyst, the best WGS kinetic model was given by Equation V.3–30, which contained mass action kinetics in the numerator and the denominator proposed by Huff and Satterfield from FT kinetics. The activation energies based on the first order in CO rate constants for the WGS reaction were 132–136 kJ / mol for the 100 Fe/0.3 Cu/0.2 K, 100 Fe/0.3 Cu/0.5 K and Ruhrchemie catalysts.

NOMENCLATURE

a	=	H_2O adsorption coefficient, Equations V.3–6, V.3–20, V.3–21, V.3–32
b	=	H_2O adsorption coefficient, Equations V.3–15, V.3–30 (MPa)
c	=	CO_2 adsorption coefficient, Equations V.3–19, V.3–20, V.3–32
$C_{l,j}$	=	Liquid phase concentration of species j (mol / ℓ)
E	=	Activation energy (kJ / mol)
f_{H_2+CO}	=	Fractional H_2–CO conversion
H_j	=	Henry's Law constant for species j (mol / $\ell \cdot$ MPa)
k_0	=	FT rate constant, Equations V.3–6, V.3–15, V.3–19, V.3–20 (mol / g–cat·h · MPa)
k_1	=	FT first order rate constant, Equation V.3–5 (mol / g–cat·h · MPa)
k_f	=	Rate constant of forward Equation V.3–22 (mol / g–cat·h · MPa)
k_{-f}	=	Rate constant of reverse Equation V.3–22 (mol / g–cat·h · MPa)
k_r	=	Rate constant of forward Equation V.3–23 (mol / g–cat·h · MPa)
k_{-r}	=	Rate constant of reverse Equation V.3–23 (mol / g–cat·h · MPa)
k_w	=	WGS first order rate constant, Equation V.3–25 (mol / g–cat·h · MPa)
$k_{w,0}$	=	WGS rate constant, Equations V.3–21, V.3–30, V.3–31, and V.3–32 (mol / g–cat·h)
K_1	=	Equilibrium constant defined by Equation V.3–12
K_2	=	Equilibrium constant defined by Equation V.3–16 (MPa^{-1})
K_j	=	Adsorption equilibrium constant, Equation V.3–7 (MPa^{-1})
K_P	=	WGS equilibrium constant, Equations V.3–21, V.3–24, V.3–30, V.3–31, and V.3–32
m	=	Average number of hydrogen atoms per product molecule, Equation V.3–1
n	=	Average carbon chain length of product molecule, Equation V.3–1
N	=	Total number of data points
P_j	=	Partial pressure of species j (MPa)
P_S	=	Standard pressure (0.101 MPa)
R	=	Gas constant ($8.314 \cdot 10^{-3}\ell$–MPa / mol · K)
R^2	=	Correlation coefficient
r_k	=	Rate of reaction k (mol / g–cat·h)
$(-r_{H_2-CO})$	=	Rate of syngas disappearance (mol / g–cat·h)
RMSE	=	Normalized root mean square error, Equation V.3–28
s	=	Space velocity (Nℓ / g–cat·h)
T_S	=	Standard temperature (273 K)
U	=	H_2/CO usage ratio

Subscripts

avg	=	Average value
FT	=	Fischer–Tropsch
i	=	Data point index
j	=	Species index (j = C_nH_m, CO, CO_2, H_2, or H_2O)
k	=	Reaction index (k = FT or WGS)
WGS	=	Water–gas shift

Superscripts

calc	=	Calculated value
d	=	Dissociative adsorption
meas	=	Measured value